



OPEN ACCESS

EDITED BY

Christiane Susanne Hampe, University of Washington, United States

REVIEWED BY

Marie Ynez Davis, University of Washington, United States Mario U. Manto, University of Mons, Belgium

*CORRESPONDENCE

Shuang Zhang,

☑ zhangshuang@nxmu.edu.cn
Xunlun Sheng,

shengxunlun@163.com

[†]These authors have contributed equally to this work and share first authorship

RECEIVED 27 August 2025 REVISED 26 October 2025 ACCEPTED 29 October 2025 PUBLISHED 14 November 2025

CITATION

Xiao P, Gu Y, Qi X, Li T, Zuo T, Xie Y, Zhang S and Sheng X (2025) Novel variant in *PNPLA6* gene causes Oliver-McFarlane syndrome in a Chinese family: 13 years follow-up . *Front. Genet.* 16:1693876. doi: 10.3389/fgene.2025.1693876

COPYRIGHT

© 2025 Xiao, Gu, Qi, Li, Zuo, Xie, Zhang and Sheng. This is an open-access article distributed under the terms of the Creative Commons Attribution License (CC BY). The use, distribution or reproduction in other forums is permitted, provided the original author(s) and the copyright owner(s) are credited and that the original publication in this journal is cited, in accordance with accepted academic practice. No use, distribution or reproduction is permitted which does not comply with these terms.

Novel variant in *PNPLA6* gene causes Oliver-McFarlane syndrome in a Chinese family: 13 years follow-up

Panpan Xiao^{1,2†}, Yonghua Gu^{1,2†}, Xiaolong Qi¹, Ting Li^{1,2}, Tingting Zuo¹, Yule Xie¹, Shuang Zhang^{2*} and Xunlun Sheng^{2,3*}

¹People's Hospital of Ningxia Hui Autonomous Region, Ningxia Medical University, Yinchuan, China, ²Ningxia Eye Hospital, People's Hospital of Ningxia Hui Autonomous Region, Yinchuan, China, ³Refractive Surgery Department, Gansu Aier Ophthalmology and Optometry Hospital, Lanzhou, China

Introduction: Oliver-McFarlane syndrome (OMCS) is a rare autosomal recessive disorder characterized by trichomegaly, severe chorioretinal dystrophy, and multiple pituitary hormone deficiencies. Its marked genetic and clinical heterogeneity presents significant challenges for definitive diagnosis.

Methods: In this study, we initially evaluated a proband clinically diagnosed with OMCS, followed by genetic analysis using whole-exome sequencing (WES). Candidate pathogenic variants were validated via Sanger sequencing and familial co-segregation analysis.

Results: WES identified compound heterozygous variants in the *PNPLA6* gene: a known missense variant (c.3241G>A, p.Gly1081Arg) and a novel missense variant (c.3461G>A, p.Arg1154His). Over a 13-year follow-up, multisystem involvement was observed, including progressive retinochoroidopathy, trichomegaly, growth retardation, and intellectual disability. Disease progression was evident, with severe exacerbation of retinochoroidopathy accompanied by newly developed pituitary hormone deficiencies and absent secondary sexual characteristics.

Discussion: Our findings expand the pathogenic variant spectrum and clinical phenotypic landscape of OMCS. Given the early onset and progressive nature of retinal involvement, we propose that early intervention targeting the preservation of retinal pigment epithelium (RPE) and photoreceptor function may be clinically beneficial.

KEYWORDS

PNPLA6, Oliver-McFarlane syndrome, trichomegaly, multiple pituitary hormone deficiencies, chorioretinal dystrophy, night blindness, retinitis pigmentosa

1 Introduction

Oliver-McFarlane syndrome (OMCS; MIM #275400) is a rare autosomal recessive disorder characterized by congenital trichomegaly, severe chorioretinal dystrophy, and multiple pituitary hormone deficiencies-including growth hormone (GH), gonadotropins (luteinising hormone, [LH] and follicle-stimulating hormone [FSH]), and thyroid-stimulating hormone (TSH) (Lisbje et al., 2021). With an estimated prevalence of <1/1,000,000, affected individuals typically present with congenital trichomegaly and elongated eyebrows, develop night blindness and visual impairment before age 5, and exhibit progressive endocrine deficits during adolescence (Lisbje et al., 2021; Hufnagel et al., 2015). These endocrine abnormalities lead to intellectual disability, visual impairment,

delayed bone age, and growth retardation, underscoring the need for specific diagnosis in patients with multisystem involvement.

Historically, OMCS diagnosis relied on clinical presentation. Advances in genetic sequencing have revealed that all reported OMCS cases arise from pathogenic variants in PNPLA6 gene (Patatin-like phospholipase domain-containing 6; MIM *603197). This gene encodes neuropathy target esterase (NTE) and is associated with a phenotypic continuum encompassing several syndromes, including: Boucher-Neuhauser syndrome (BNS; MIM #215470), Gordon-Holmes syndrome (GHS; MIM #212840), Oliver-McFarlane syndrome (OMCS; MIM, #275400), Lawrence-moon syndrome (LMS; MIM #245800) and spastic paraplegia type 39 (SPG39; MIM #612020) (OMIM, 2025). These disorders share variable combinations of cerebellar ataxia, upper motor neuron involvement, chorioretinal dystrophy, and hypogonadotropic hypogonadism. Specifically: BNS features cerebellar ataxia, chorioretinal dystrophy and hypogonadotropic hypogonadism. GHS presents with cerebellar ataxia, hypogonadotropic hypogonadism, and brisk reflexes OMCS is defined by trichomegaly, chorioretinal dystrophy, short stature, intellectual disability, and hypopituitarism LMS SPG39 involve upper motor neuron signs, peripheral neuropathy, and occasionally cognitive impairment and/or cerebellar ataxia (Synofzik et al., 2014). No consistent genotypephenotype correlations have been established for PNPLA6-related disorders. To date, the Human Gene Mutation Database (HGMD) documents 109 pathogenic PNPLA6 variants (https://www.hgmd. cf.ac.uk/ac/gene.php?gene=PNPLA6; accessed June 2025). Elucidating PNPLA6 's role in multisystem disorders may yield novel therapeutic insights.

Here, we present a 13-year follow-up of a Chinese patient with OMCS, who was initially diagnosed at age 5 with clinical features of trichomegaly, scalp hair thinning, thickened eyebrows, chorioretinal dystrophy, retinitis pigmentosa, visual impairment, and growth delay. Clinical diagnosis of OMCS was based on these findings; however, genetic confirmation was not achievable due to technical constraints at that time. During the untreated follow-up period, the proband developed progressive chorioretinal dystrophy, retinitis pigmentosa, multiple pituitary hormone deficiencies, and abnormal secondary sexual characteristics. Subsequent genetic testing identified a novel compound heterozygous *PNPLA6* variant, expanding the known genotype-phenotype spectrum of OMCS. This finding enriches the variant database for OMCS, and provides valuable support for research into its multisystem pathogenesis.

2 Methods

2.1 Data collection

A family affected by OMCS was recruited through the Ningxia Eye Hospital at the People's Hospital of Ningxia Hui Autonomous Region. The pedigree spanned two generations and included four family members, including one affected individual. Detailed histories, covering family structure, marital status, reproductive outcomes, and medical background, were obtained from the proband and parents. Based on this information, a pedigree chart

was constructed. Both comprehensive physical examinations and specialized ophthalmic assessments were performed on the affected individual.

This study received approval from the Ethics Committee of the People's Hospital of Ningxia Hui Autonomous Region (Approval No. 2021-KJHM-014) and strictly adhered to the principles of the *Declaration of Helsinki*. Informed consent was secured from all participants, including the proband—a special school student with preserved basic daily living skills and without significant functional impairment.

2.2 Clinical examination

The proband (Figure 1a, II:1), a 18-year-old male born to nonconsanguineous healthy parents (I:1, I:2) with a healthy older (II:2),underwent comprehensive clinical ophthalmological evaluation. The clinical assessment included cranial magnetic resonance imaging (MRI), hand radiography, Denver Developmental Screening Test, and laboratory analyses (complete blood count, fasting glucose, hepatic/renal function, lipid profile, hepatitis B screening, and comprehensive endocrine panel). Ophthalmological examinations comprised: bestcorrected visual acuity (BCVA) assessment using a Snellen chart and VT-10 autorefractor (Topcon, Japan); intraocular pressure (IOP) measurement; slit-lamp examination; axial length measurement (IOL Master 500, Carl Zeiss Meditec AG); color fundus photography (TRC-NW300; Topcon, Japan); fullfield electroretinography (ff-ERG) with corneal jet electrodes (RetiPort ERG; Roland Consult, Germany) following the standards of the International Society of Clinical Electrophysiology of Vision (ISCEV); visual fields (VF) testing (Humphrey Field Analyzer 750i, Carl Zeiss Meditec, United States; 30-2 protocol: 30°field, 76-point grid, 31.5 asb background); and Spectral-domain optical coherence tomography (SD-OCT; Cirrus HD-OCT4000, Carl Zeiss Meditec, United States) with macular cube (512 × 128) and HD 5-line raster scans through the foveal center. Bilateral mydriasis was induced using 0.5% tropicamide ophthalmic solution prior to posterior segment imaging.

2.3 Genetic testing and analysis

WES was performed on peripheral blood samples from the proband and family members. Genomic DNA was extracted, and libraries prepared. Target regions, including exons, adjacent splice sites (±20 bp), and the mitochondrial genome, were captured and enriched via probe hybridization. Following quality control, high-throughput sequencing was conducted. Quality-filtered reads were aligned to the hg38 human reference genome using Bio-BWA software. Single nucleotide variants (SNVs) and insertions/deletions (InDels) were called using GATK haplotypeCaller, then annotated and filtered using clinical databases and bioinformatics tools. Variant interpretation adhered to the guidelines of the American College of Medical Genetics and Genomics (ACMG) and the recommendations of the ClinGen Sequence Variant

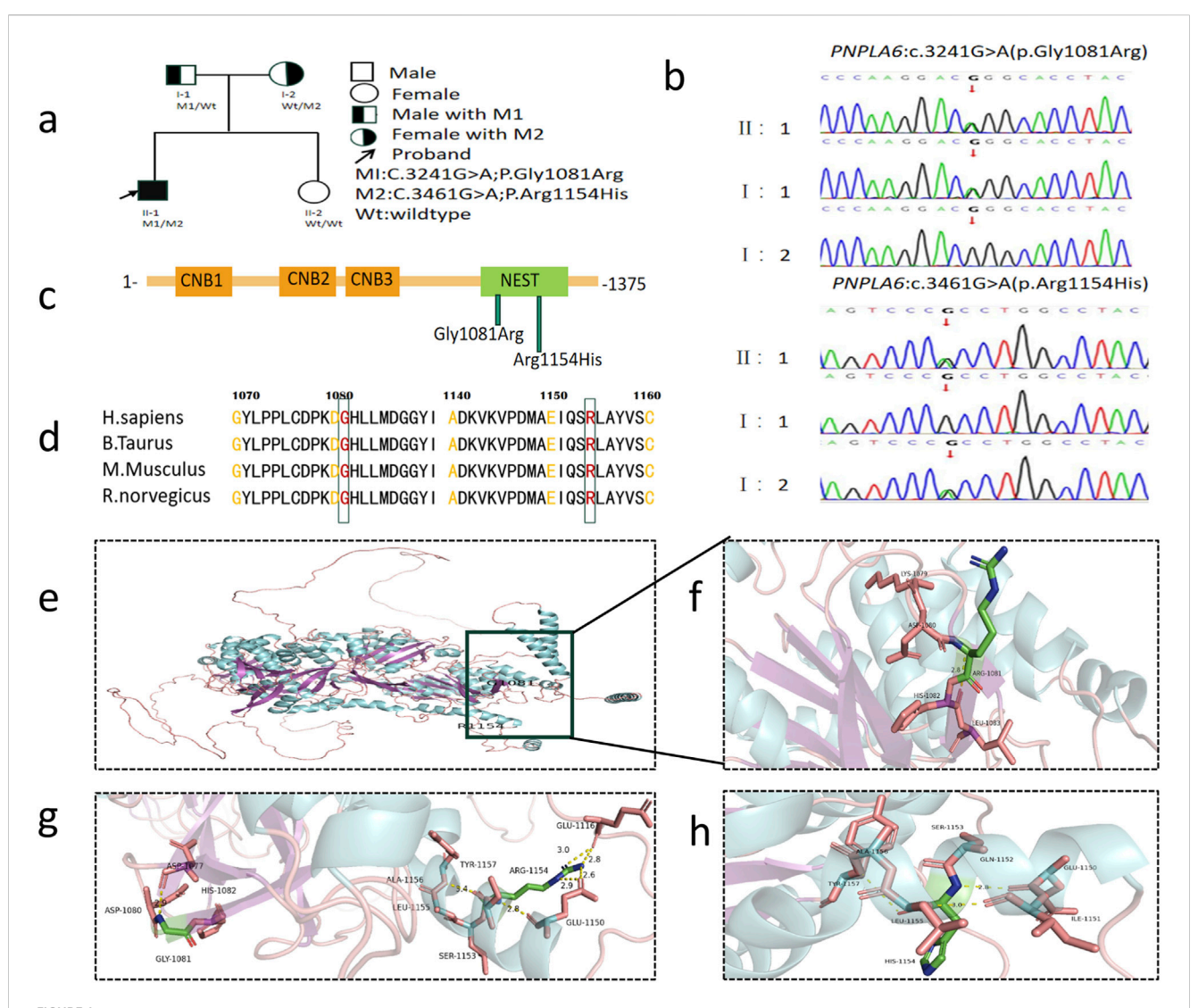


FIGURE 1
Genetic findings in the family with OMCS. (a) Pedigree of the family. The filled black symbols represent the affected member and the arrow denotes the proband. (b) By sequencing analysis, compound heterozygous variants of (c) 3241G>A and (c) 3461G>A were identified in the proband (II:1). (c) The PNPLA6 protein structure includes three cyclic nucleotide binding (CNB) domains and a C-terminal patatin-like catalytic domain (NEST). (d) The homology of amino acid sequences between human PNPLA6 and other species. The amino acid at position 1,081 (Glycine, Gly1081) and at position 1,154 (Arginine, Arg1154) are highly conserved among species. (e) Overall structure diagram of wild-type PNPLA6 protein. (f) Local structure diagram of wild-type PNPLA6 protein. (g) Gly1081Arg mutation local structure map. (h) Arg1154His mutation local structure map.

Interpretation (SVI) working group (Richards et al., 2015). Cosegregation analysis was performed via Sanger sequencing in family members.

2.4 In silico analysis

Identified variants were screened against the HGMD to check for previously reported pathogenicity. Pathogenicity assessment followed ACMG guidelines, classifying variants into five categories: pathogenic, likely pathogenic, uncertain significance, likely benign and benign. Evolutionary conservation was analyzed using UniProt. Computational pathogenicity predictions were generated using PolyPhen-2, MutationTaster, and FATHMM-MKL. The wild-type PNPLA6 protein structure was modeled

using SWISS-MODEL, with mutant conformations visualized in PyMol.

3 Results

3.1 History and clinical manifestations of the proband

The proband, born to healthy non-consanguineous parents without a family history of stillbirth, intellectual disability, or congenital anomalies, presented to Ningxia Eye Hospital at 5 years of age with night blindness. Neonatal parameters (weight, length, head circumference) were within normal ranges (Li et al., 2009). At the initial assessment, the proband measured 102 cm in

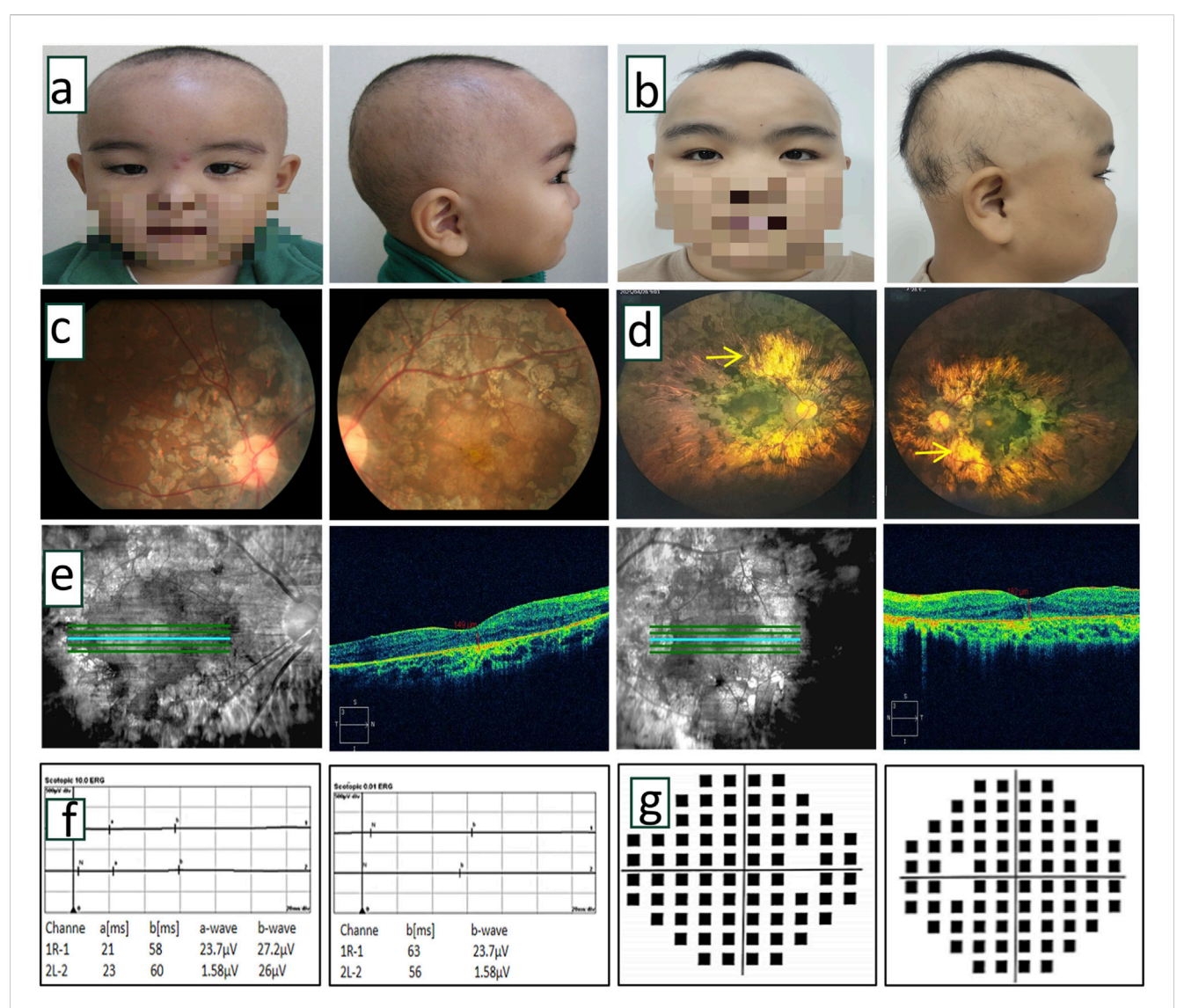


FIGURE 2
Clinical examination of proband. (a,b) Front and side photos of the proband at 5 years old and 18 years old. The proband exhibited sparse hair, thick eyebrows, and long, upward-curled eyelashes (trichomegaly). (c) Color fundus photographs of the proband at the age of 5 years indicated obvious chorioretinal dystrophy with retinitis pigmentosa in both eyes. (d) The laser scanning fundus images of the proband after 13 years of follow-up showed a clear boundary of the optic disc in both eyes, light red color, no obvious optic cup, extensive uneven chorioretinal dystrophy with retinitis pigmentosa, and partial porcelain white sclera visible in the posterior pole (\rightarrow indicated). (e) OCT scanning images of the proband at 13 years follow-up indicated thinning of retinal tissue structure, absence of ellipsoid band, uneven reflection signal of retinal pigment epithelium, and uneven degeneration of choroid membrane. (f) After 13 years of follow-up, ERG showed that a wave and b wave disappeared in the 10.0 response of ocular dark adaptation, showing an extinction type. Binocular dark adaptation 0.01 showed the disappearance of b wave, which showed the extinction type. (g) After 13 years of follow-up, visual field testing showed severe visual field defects in both eyes.

height (<10th percentile) and weighed 18.5 kg (between the 25th and 50th percentile). Hand X-ray bone age assessment revealed delayed skeletal maturation. With the proband presenting sparse scalp hair, thick eyebrows, and trichomegaly (Figure 2a) (Sheng et al., 2015), no remarkable abnormalities were observed in the other family members. Cranial MRI showed unremarkable neuroanatomy. Neurological evaluation demonstrated intact motor function, coordination, tendon reflexes, and muscle tone. The Denver Developmental Screening Test indicated minor deficits in gross motor and language domains. Funduscopic examination revealed bilateral retinochoroidopathy with patchy atrophy and retinal pigmentary degeneration (Figure 2c) (Sheng et al., 2015).

Follow-up at 18 years of age, the proband's height was 158 cm (<10th percentile) and weight was 60 kg (between the 50th and 75th percentile). Physical characteristics included thick eyebrows, sparse scalp hair, trichomegaly, abnormal secondary sexual characteristics (micropenis, absent Adam's apple, and absence of pubic and axillary hair), gait instability with frequent falls, dyspraxia (inability to carry basins without spilling), and impaired coordination (inability to maintain a single-leg stance) (Figure 2b). The neurological physical examination revealed no obvious abnormalities. However, a comprehensive neurophysiological assessment (including electroencephalogram, and visual evoked potentials) could not be completed as the patient and the family

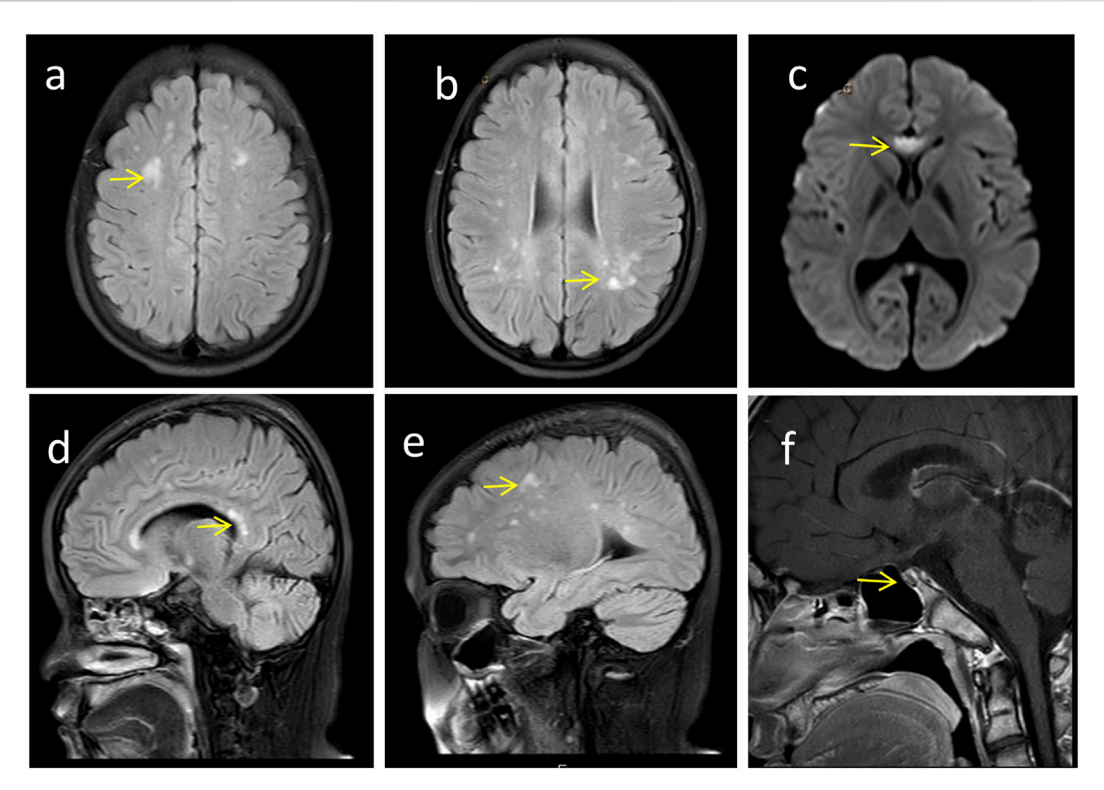


FIGURE 3 Craniocerebral imaging findings of the proband. (a-e) Brain MRI reveals high-signal white matter lesions (\rightarrow indicated), which involve the bilateral centrum semiovale, periventricular regions, as well as the genu and splenium of the corpus callosum. (f) Enhanced MRI of the pituitary gland demonstrates pituitary atrophy (\rightarrow indicated).

declined these tests. Cranial MRI (Figures 3a–e) showed T2-WI/T2-FLAIR hyperintense white matter lesions (Fazekas II) in the bilateral centrum semiovale, periventricular regions, and genu/splenium of the corpus callosum. Callosal lesions appeared slightly hypointense on T1WI and hyperintense on DWI. Pituitary MRI with contrast (Figure 3f) revealed a sagittal height of 2.5 mm, consistent with pituitary atrophy.

Laboratory investigations revealed significant abnormalities in endocrine parameters. Hormonal assays showed decreased levels of LH, GH, prolactin (PRL), progesterone (P), testosterone (T), and free thyroxine (FT4), along with elevated insulin levels. Additionally, hematological and metabolic abnormalities were observed, including an abnormal red cell distribution width (RDW), derangements in the complete blood count (white blood cell count [WBC], hematocrit), hyperuricemia, abnormal liver function (aspartate aminotransferase [AST], AST/ALT ratio) and lipid profile abnormalities (elevated triglycerides, low high-density lipoprotein cholesterol [HDL-C].

Ophthalmic evaluation revealed bilateral high myopia with BCVA of 0.01 (with a -6.00 spherical equivalent refractive correction) in oculus dexter (OD) and 0.05 (with a -6.25 spherical equivalent refractive correction) in oculus sinister (OS). Axial length measurements were 23.10 mm (OD) and 23.11 mm (OS). He showed bilateral horizontal nystagmus without obvious squint. Slit-lamp biomicroscopy showed normal anterior segment. Fundoscopy revealed well-defined, light red optic discs with absent cupping, extensive patchy chorioretinal dystrophy with retinitis pigmentosa, and posterior pole exposure

of porcelain-white sclera (Figure 2d). OCT demonstrated retinal thinning, loss of the ellipsoid zone, and irregular chorioretinal atrophy (Figure 2e). VF testing showed severe bilateral constriction (Figure 2g). ff-ERG showed extinguished waveforms (absent a- and b-waves), confirming severe chorioretinal dystrophy (Figure 2f).

3.2 Genetic test results

WES identified compound heterozygous variants in the PNPLA6 gene of the proband (Figure 1a, II:1): a known missense variant (M1) and a novel missense variant (M2) (Figure 1a). The PNPLA6 protein structure contains three cyclic nucleotide binding (CNB) domains and a C-terminal patatin-like catalytic domain (NEST). Both M1 and M2 mutations are located within the NEST (Figure 1c). Sanger sequencing confirmed the segregation pattern: the proband and father (I:1) carried the M1 variant, while the proband and mother (I:2) harbored the M2 variant (Figure 1b). At base pair 3,241 of the PNPLA6 gene, the M1 variant results in a guanine (G) to adenine (A) substitution, leading to the replacement of glycine (Gly) with arginine (Arg) at position 1,081 in the protein-coding sequence. This disrupts the original hydrogen bond between Gly1081 and Asp1080, increasing positive charge and reducing hydrophobicity at residue 1,081. Similarly, at base pair 3,461, the M2 variant involves a guanine (G) to adenine (A) substitution, replacing arginine (Arg) with histidine (His) at position 1,154 in the protein-coding sequence.

TABLE 1 The effects of PNPLA6 variations on their protein function by in silico analysis.

Variants	Software	Score	Predicted signal
c.3241G>A (p.Gly1081Arg)	Mutation taster	1.0	Disease causing
c.3461G>A (p.Arg1154His)	Mutation taster	1.0	Disease causing
c.3241G>A (p. Gly1081Arg)	PolyPhen-2	1.0	Damaging
c.3461G>A (p. Arg1154His)	PolyPhen-2	1.0	Damaging
c.3241G>A (p. Gly1081Arg)	fathmm-MKL	0.99199	Damaging
c.3461G>A (p. Arg1154His)	fathmm-MKL	0.99553	Damaging

This abolishes the hydrogen bond between Arg1154 and Glu1116, decreasing positive charge and enhancing hydrophobicity at residue 1,154 (Figures 1e-h). The M1 variant has a population frequency of 0 in the gnomAD_EAS database, while M2 is absent from gnomAD and unreported in the literature or genomic databases, supporting its novelty. Phylogenetic conservation analysis revealed high evolutionary conservation at residues 1,081 and 1,154 across species (Figure 1d), indicating critical roles in PNPLA6 function. Both variants were bioinformatically predicted to be deleterious (Table 1). According to ACMG guidelines, M1 was categorized as a likely pathogenic (LP = PS3+PM3+PM2+PP3+PP4), and M2 as likely pathogenic (LP = PM2+PM3+PP3+PP4) (Table 2). Collectively, the compound heterozygous variants in the PNPLA6 gene likely disrupt function, contributing to protein structure and pathogenesis of OMCS.

4 Discussion

4.1 The evolution of clinical manifestations in this case of OMCS

We present a 13-year longitudinal follow-up of an OMCS case with novel genetic associations. Clinical diagnosis was established at age five based on characteristic features: chorioretinal dystrophy, retinitis pigmentosa, growth delay, trichomegaly (presenting as elongated curly eyelashes and thick eyebrows), and sparse scalp hair. Subsequent monitoring revealed persistent developmental delays, short stature, and gross motor dysfunction. Without therapeutic intervention, retinochoroidopathy progressively worsened, leading to a decreased BCVA. Concurrently, the patient developed endocrine deficiencies during adolescence, including absence of secondary sexual characteristics. Laboratory analysis confirmed deficiencies in LH and GH, while FSH and TSH levels remained within normal ranges. Neuroimaging confirmed pituitary atrophy.

4.2 Clinical phenotypic features of OMCS

First described in 1965, OMCS is a rare autosomal recessive disorder caused by pathogenic variants in the *PNPLA6* gene. Its core clinical manifestations include trichomegaly, severe chorioretinal dystrophy, and combined pituitary hormone deficiencies (GH, TSH, LH/FSH) (Patsi et al., 2018; Liu et al., 2020). Our systematic review of 36 published cases (Table 3) showed that trichomegaly (35/36,97%) and chorioretinal dystrophy (36/36,100%) are universal features, while GH deficiency (25/36, 69%), gonadotropin deficiency (24/36,67%), delayed bone age (27/36, 75%), and hair abnormalities (26/36, 72%) are highly prevalent. Approximately half of the patients exhibit TSH deficiency (16/36,44%), and neurological symptoms (21/36,58%). Collectively, these findings establish trichomegaly,

TABLE 2 Pathogenicity analysis of variants by ACMG.

Variants of PNPLA6	Evidence of pathogenicity
NM_006702,5: exon30: c.3241G>A	a. Functional studies have been supportive of a damaging effect on the gene or gene product for this variant. (PS3_Moderate). b. It has been reported that pathogenic variant p.R1031fs+38 has been detected in the trans of this variant (PM3). c. This variant is a rare variant with a frequency of 0 in the general East Asian population in gnomAD database (PM2_Supporting). d. Multiple bioinformatics software predicted deleterious effects of the mutation on genes or gene products (PP3) e. Proband's proband's phenotype is highly specific for Oliver-McFarlane syndrome with a single genetic etiology (PP4)
NM_006702.5: exon31: c.3461G>A	a. This mutation is a rare variation and was not included in the general East Asian population in gnomAD database. (PM2_Supporting) b. This variant was located in the trans of the likely pathogenic variant M2 (c.3461G>A: p. Arg1154His) (PM3). c. Multiple bioinformatics software predicts harmful effects of the variant on genes or gene products (PP3) d. proband's phenotype is highly specific for Oliver-McFarlane syndrome with a single genetic etiology (PP4)

ACMG, Standards and Guidelines for Interpretation of Sequence Variants issued by American College of Medical Genetics and Genomics (ACMG) in 2015.

TABLE 3 Characteristics of Oliver-McFarlane cases previously described in the literature.

Author	Sex	Birth weight(g)	Bone age	Trichomegaly	Retinopathy	Hair	GH deficiency	Hypothyroidism	Hypogonadism	Mental retardation	Neurological involvement	Variation 1	Variation 2
Oliver and McFarlane. (1965)	M	1800	Delayed	+	+	Sparse	_	+	_	+	NA	NA	NA
Cant	F	2500	Delayed	+	+	Alopecia	+	_	+	_	Neuropathy	NA	NA
Sampson et al. (1989)	F	2500	Delayed	+	+	Alopecia	+	_	+	_	Neuropathy	NA	NA
Corby et al. (1971)	M	2000	Delayed	+	+	Sparse	_	_	_	+	NA	NA	NA
Zaun et al. (1984)	F	1700	Delayed	+	+	Alopecia	_	_	_	_	_	NA	NA
Zaun et al. (1984)	M	2600	Delayed	+	+	Sparse	_	+	+	+	Ataxia	NA	NA
Patton et al. (1986)	M	NA	Delayed	+	+	Alopecia	+	+	+	Mild	Ataxia,spastic,paraplegia, Neuropathy	p.(Arg983Glnfs*38) c.2944_2947dupAGCC	p.(Gly1081Arg) c.3241G>A
Hufnagel et al. (2015)	M	NA	Delayed	+	+	Alopecia	+	+	+	Mild	Ataxia,spastic,paraplegia, Neuropathy	p.(Arg983Glnfs*38) c.2944_2947dupAGCC	p.(Gly1081Arg) c.3241G>A
Matheieu et al. (1991)	M	3110	Delayed	+	+	Alopecia	_	_	+	Mild	Peripheral	NA	NA
Matheieu et al. (1991)	M	2400	Delayed	+	+	_	+	_	+	_	neuropathy	NA	NA
Haritoglou et al. (2003)	M	2220	Delayed	+	+	Sparse	NA	_	+	+	_	NA	NA
Haimi and Gershoni—Baruch. (2005)	M	1560	Delayed	+	+	Sparse	+	_	+	Mild	Ataxia, neuropathy	NA	NA
Haimi and Gershoni—Baruch. (2005)	F	1951	Delayed	+	+	Sparse	+	_	_	Mild	_	NA	NA
Somnez et al. (2008)	M	2360	NA	+	+	_	+	+	+	+	Neuropathy	NA	NA
Luiz Pedroso et al. (2014)	F	NA	NA	+	+	Alopecia	NA	NA	+	NA	Ataxia	NA	NA
Kmoch et al. (2015)	F	2000	Delayed	+	+	_	+	+	_	_	_	p.(Leu476Pro) c.1427T>C	p.(Asp1077Asn) c.3229G>A
Kmoch et al. (2015)	M	NA	NA	+	+	Sparse	+	+	_	_	Neuropathy and/or ataxia	p.(Gln658*) c.1972C>T	p.(Gly1081Arg) c.3241G>C
Kmoch et al. (2015)	F	3000	NA	+	+	Alopecia	+	_	+	_	Neuropathy and/or ataxia	c.199–2A>T	p.(Asp1077Asn) c.3229G>A
Kmoch et al. (2015)	F	3300	NA	+	+	_	+	_	+	_	Neuropathy and/or ataxia	c.199-2A>T	p.(Asp1077Asn) c.3229G>A

TABLE 3 (Continued) Characteristics of Oliver-McFarlane cases previously described in the literature.

Author	Sex	Birth weight(g)	Bone age	Trichomegaly	Retinopathy	Hair	GH deficiency	Hypothyroidism	Hypogonadism	Mental retardation	Neurological involvement	Variation 1	Variation 2
Kmoch et al. (2015)	M	1900	NA	+	+	Alopecia	+	_	+	_	Neuropathy and/or ataxia	c.199-2A>T	p.(Asp1077Asn) c.3229G>A
Kmoch et al. (2015)	F	2500	Delayed	+	+	Alopecia	+	+	+	Mild	Neuropathy and/or ataxia	p.(Arg1060Trp) c.3178C>T	p.(Gly1081Arg) c.3241G>C
Kmoch et al. (2015)	F	2500	Delayed	_	+	Alopecia	+	+	+	_	Neuropathy	p.(Leu366Serfs*28) c.1094dup	p.(Gly1081Arg)c.3241G>C
Kmoch et al. (2015)	M	2400	Delayed	+	+	NA	+	+	+	+	Neuropathy and/or ataxia	p.(Trp873*) c.2619G>A	NA,only one variant
Hufnagel et al. (2015)	F	2555	Delayed	+	+	Sparse	+	+	NA	_	_	p.(Arg1051Gln) c.3152G>A	p.(Gly1128Ser) c.3382G>A
Hufnagel et al. (2015)	M	2612	Delayed	_	+	Sparse	+	+	NA	_	_	p.(Arg1051Gln) c.3152G>A	p.(Gly1128Ser) c.3382G>A
Hufnagel et al. (2015)	M	NA	Delayed	+	+	_	+	+	NA	_	Neuropathy	p.(Arg983Glnfs*38) c.2944_2947dupAGCC	p.(Gly1081Arg) c.3241G>A
Hufnagel et al. (2015)	M	NA	NA	+	+	Alopecia	+	_	+	_	_	c.1829+2T>G	p.(Val1167Ala) c.3500T>C
Hufnagel et al. (2015)	M	NA	Delayed	+	+	_	+	+	NA	_	_	dup(ex14_20)	p.(Val1167Ala) c.3500T>C
Patsi et al. (2018)	F	NA	NA	+	+	Sparse	+	+	+	NA	Ataxia, neuropathy	p.(Ser1159Tyr) c.3476C>A	p.(Ser1159Tyr) c.3476C>A
Makuloluwa et al. (2020)	F	2980	Delayed	+	+	_	_	_	_	_	_	p.(Ala1064Thr) c.3190G>A	p.(Arg1135Trp) c.3403C>T
Liu et al. (2020)	М	1900	NA	+	+	NA	NA	+	+	+	Seizures	p.(Gln497His) c.1491G>T	p.(Gly1123Arg) c.3367G>A
Wu et al. (2021)	M	NA	Delayed	+	+	Sparse	+	NA	+	_	_	p.(Ser997Leu) c.2990C>T	c.3702 + 1G>A
Kristian et al	F	1650	Delayed	+	+	Sparse	+	_	NA	_	_	p.(Arg277Pro) c.830G>C	p.(Gly1081Arg) c.3241G>A
Kristian et al	M	1430	Delayed	+	+	Sparse	+	_	+	_	_	p.(Leu366Serfs*28) c.1094dup	p.(Asp1147Glu) c.3441C>G
Shi et al. (2023)	F	NA	Delayed	+	+	_	NA	_	+	NA	Neuropathy and/or ataxia	p.(Asp1141Gly) c.3342A>G	p.(Phe338Leufs*80) c.1094dup
Our case	M	2950	Delayed	+	+	Alopecia	_	_	+	Mild	_	p.(Gly1081Arg) c.3241G>A	p.(Arg1154His) c.3461G>A

M, malen; F, female, +: Present, -: not presen; NA, informaton not available; GH, growth hormone.

chorioretinal dystrophy, GH deficiency, and gonadotropin deficiency as cardinal features of OMCS.

4.3 Trichomegaly in OMCS

Trichomegaly-characterized by abnormal lengthening, thickening, curling, or pigmentation of eyelashes-is a hallmark of OMCS. Although eyelash trichomegaly may be drug-induced, surgery-related, or associated with other conditions, its pathogenesis in OMCS is thought to involve dysregulated hair follicle biology (Hutchison et al., 2022). Epidermal growth factor receptors (EGFR), highly expressed in the proliferative, undifferentiated outer root sheath of hair follicles, play a crucial role in hair growth, as evidenced by the hair growth inhibition observed with EGFR antagonists. Additionally, prostaglandins can transition hair follicles from telogen (resting) to anagen (growth) phase (Lacouture et al., 2006; Dueland et al., 2003). Studies suggest that trichomegaly is associated with elevated levels of phosphatidylethanolamine in follicular cells, which promotesincreased prostaglandin production and abnormal eyelash growth (Yamamoto et al., 2011). However, the exact mechanisms in OMCS remain incompletely understood.

4.4 Chorioretinal dystrophy

Chorioretinal dystrophy is a core feature of PNPLA6-related OMCS, presenting as progressive vision loss, visual field defects, and characteristic fundus changes, typically with onset before 5 years of age. Funduscopy reveals diffuse chorioretinal atrophy and pigment clumping, OCT demonstrates retinal thinning, loss of the layered architecture, RPE depletion, and choriocapillaris loss (Doğan et al., 2021). In our proband, persistent choroidal and retinal atrophy was observed. The pathophysiology may involve the loss of phospholipase B (PLB) activity caused by PNPLA6 variants. PNPLA6 facilitates choline transfer from RPE cells to photoreceptors, thereby supporting their survival. An impaired choline supply leads to abnormal morphology, proliferation, metabolism, and function of RPE and photoreceptor cells, contributing to visual deterioration and retinal degeneration (Ono et al., 2025). Although no validated treatment has been reported to reverse retinal damage, early intervention aimed at preserving RPE and photoreceptor function may be beneficial, given the early onset and progressive nature of retinal involvement.

4.5 Pituitary hormone deficiencies and neurological manifestations

Combined pituitary hormone deficiencies contribute to developmental delays and abnormal secondary sexual characteristics in OMCS. GH/LH deficiencies, as seen in our proband, can lead to impaired pubertal development, including micropenis, small testes, sparse facial hair, high-pitched voice, and lack of voice breaking (Nedresky and Singh, 2022). In this study, low GH and LH levels, compounded by the patient's refusal of

hormone replacement therapy, may have exacerbated growth retardation and abnormal sexual development.

Neurological and imaging abnormalities are also reported in *PNPLA6*-related disorders, including white matter signal changes, pituitary and cerebellar atrophy, and empty sella turcica. These may arise from loss of NTE function, leading to endoplasmic reticulum damage, vacuolation of nerve cell bodies, and abnormal reticular aggregates in the nervous system. NTE plays a crucial role in maintaining intracellular phospholipid homeostasis. Therefore, *PNPLA6* variants may cause neurodegeneration via NTE dysfunction (Topalogl et al., 2014; Akassoglou et al., 2004). In our proband, cranial MRI showed hyperintense white matter signals involving the bilateral centrum semiovale, periventricular areas, and corpus callosum (genu and splenium), along with pituitary atrophy. White matter changes may underlie gait and balance impairments, while pituitary atrophy likely contributes to hormone deficits.

Multidisciplinary evaluation (ophthalmology, neurology, endocrinology) and genetic testing improve diagnostic accuracy for OMCS. Although no consensus on a standard treatment approach has been established, early hormone replacement therapy may mitigate developmental and intellectual impairments. Emerging strategies, including gene therapy, local choline application, and NTE activity modulation, show promise but require further validation (Shi et al., 2023; Liu et al., 2024).

4.6 Gene structure and function

PNPLA6 (Patatin-like phospholipase domain containing 6), originally termed NTE, is a member of the nine-protein patatin-like phospholipase family. Located on chromosome 19p13.2, the *PNPLA6* gene comprises 37 exons and produces five transcript variants; the longest (NM_001166111) encodes a 1,375-amino-acid protein (151 kDa) with three domains: an N-terminal transmembrane domain, three cyclic nucleotide binding (CNB) domains, and a C-terminal patatin-like catalytic domain (NEST) (Liu and Hufnagel, 2023). Among 109 reported *PNPLA6* variants (HGMD), missense/nonsense variants are most common (84/109, 77%), followed by splicing (10/109, 9.2%), small insertions/deletions/indels (12/109, 11%), and gross insertions/deletions (3/109, 2.8%). Over 50% localize to the patatin domain; missense variants within the NEST domain correlate with severe retinopathy and endocrinopathy (Liu et al., 2024).

PNPLA6 variants are linked to five clinically heterogeneous disorders: BNS, OMCS, GHS, LMS and SPG39. Although comorbid spastic paraplegia and parkinsonism have been reported in PNPLA6-related disorders, the proband in this study has not yet developed these signs, exhibiting only mild gait instability, ataxia, and coordination disorders (Kazanci et al., 2022). Given the proband's current young age, this absence could b age-dependent, which warrants long-term follow-up to monitor disease progression. Overlapping features include chorioretinopathy (in BNS, OMCS, and LMS) and cerebellar ataxia with hypogonadotropism (in GHS and SPG39) (Table 4). No correlation exists, but disease severity inversely correlates with residual NTE activity (Liu et al., 2024).

TABLE 4 PNPLA6 Disorders: Comparison of Phenotypic Clusters by Select Features. OMCS = Oliver-McFarlane syndrome; BNS = Boucher-Neuhäuser syndrome; GHS = Gordon Holmes syndrome; LMS = Laurence-Moon syndrome; SPG39 = spastic paraplegia type 39. Note: The clusters in this table do not constitute distinct phenotypes, as they may overlap in many affected individuals.

Phenotypic feature	PNPLA6 disor	ders				
	OMCS	BNS	BNS GHS		SPG39	Parkinsonian
Cerebellar ataxia		+	+	+	+	
Peripheral neuropathy				+	+	
Cognitive dysfunction					+	
Chorioretinal dystrophy	+	+		+		
Trichomegaly	+					
Hypothyroidism	+	+	+			
Hypogonadism	+	+	+			
GH deficiency	+				+	
Motor dysfunction						+

PNPLA6 is ubiquitously expressed, with high levels in the central nervous system, lymphoid tissue, kidney, lung, and testis. In the eye, it is abundant in RPE cells but minimally expressed in photoreceptors. Functionally, PNPLA6 exhibits lysophospholipase/PLB activity, hydrolyzing lysophosphatidylcholine (LPC) and phosphatidylcholine (PC) to release glycerophosphocholine (GPC), which is further metabolized into choline-critical for cellular homeostasis. In the retina, PNPLA6-mediated PC catabolism mobilizes endogenous choline, whose recycling into PC is essential for RPE and photoreceptor integrity (Richardson et al., 2020; Ono et al., 2025). Loss of PNPLA6 activity, due to pathogenic variants, disrupts choline metabolism and triggers retinal degeneration via two key pathways: ① Accumulation of PC and LPC in RPE cells, coupled with reduced choline, impairs proliferation, adhesion, phagocytosis, mitochondrial dysfunction; ② Disrupted choline secretion from RPE to photoreceptors leads to structural and functional impairment of photoreceptors due to choline deficiency. Notably, choline supplementation reverses retinal pathology in PNPLA6-deficient models: local administration of 2% choline restored retinal thickness, photoreceptor outer segment structure, and enhanced visual function in PNPLA6-deficient mice (Ono et al., 2025). This suggests choline modulation as a promising therapeutic strategy for PNPLA6associated retinopathy, though further research is needed.

While animal studies have established that *PNPLA6* variants impair NTE activity and disruptcholine metabolism to cause disease, the complete pathogenic cascade remains incompletely elucidated. Key unanswered questions include how these variants progressively compromise protein function and disrupt core cellular processes-such as signal transduction, cell cycle, cell death, and cell differentiation and how these disruptions ultimately manifest as multisystem abnormalities including chorioretinal dystrophy, neurological disorders, and endocrine dysfunction (Liu et al., 2024; Richardson et al., 2020). Future research should integrate systematic clinical follow-up with in-depth basic science to delineate the specific molecular steps and regulatory networks through which *PNPLA6* gene variants impair NTE activity and choline metabolism. Such efforts are crucial for deciphering diseases pathogenesis and will lay the necessary theoretical foundation for the developing targeted therapies.

5 Conclusion

This study identifies a novel compound heterozygous *PNPLA6* variant (c.3241G>A/c.3461G>A) in an OMCS patient, expanding the spectrum of pathogenic variants and clinical phenotypes. Long-term follow-up confirms the progressive nature of OMCS, particularly affecting RPE and photoreceptor cells and leading to chorioretinal atrophy. Early intervention aimed at preserving RPE and photoreceptor function may be beneficial, given the early onset and progressive nature of retinal involvement.

Data availability statement

The datasets for this article are not publicly available due to concerns regarding participant/patient anonymity. Requests to access the datasets should be directed to the corresponding authors.

Ethics statement

The studies involving humans were approved by the People's Hospital of Ningxia Hui Autonomous Region (Approval No. 2021-KJHM-014). The studies were conducted in accordance with the local legislation and institutional requirements. The participants provided their written informed consent to participate in this study. Written informed consent was obtained from the individual(s) for the publication of any potentially identifiable images or data included in this article.

Author contributions

PX: Writing – original draft. YG: Writing – original draft. XQ: Writing – review and editing. TL: Writing – review and editing. TZ: Writing – review and editing. YX: Writing – review and editing. SZ: Writing – review and editing.

Funding

The author(s) declare that financial support was received for the research and/or publication of this article. Ningxia Natural Science Foundation [2022AAC03388] supported the collection of clinical information. The Ningxia Science and Technology for the People Project [2022CMG03027] supported genetic testing and the publication.

Acknowledgements

The authors thank all subjects for their participation.

Conflict of interest

The authors declare that the research was conducted in the absence of any commercial or financial relationships that could be construed as a potential conflict of interest.

References

Akassoglou, K., Malester, B., Xu, J., Tessarollo, L., Rosenbluth, J., and Chao, M. V. (2004). Brain-specific deletion of neuropathy target esterase/swisscheese results in neurodegeneration. *Proc. Natl. Acad. Sci.* 101 (14), 5075–5080. doi:10.1073/pnas. 0401030101

Corby, L. D. G., Lowe, R. S., Haskins, M. R. C., and Hebertson, C. L. M. (1971). Trichomegaly, pigmentary degeneration of the retina, and growth retardation: a new syndrome originating in utero. *Am. J. Dis. Child.* 121 (4), 344–345. doi:10.1001/archpedi.1971.02100150118018

Doğan, M., Eröz, R., and Öztürk, E. (2021). Chorioretinal dystrophy, hypogonadotropic hypogonadism, and cerebellar ataxia: boucher-neuhauser syndrome due to a homozygous (c.3524C>G (p. Ser1175Cys)) variant in PNPLA6 gene. *Ophthalmic Genetics 42* (3), 276–282. doi:10.1080/13816810.2021. 1894461

Dueland, S., Sauer, T., Lund-Johansen, F., Ostenstad, B., and Tveit, K. M. (2003). Epidermal growth factor receptor inhibition induces trichomegaly. *Acta Oncol* 42 (4), 345–346. doi:10.1080/02841860310006038

Haimi, M., and Gershoni-Baruch, R. (2005). Autosomal recessive Oliver-McFarlane syndrome: retinitis pigmentosa, short stature (GH deficiency), trichomegaly, and hair anomalies or CPD syndrome (chorioretinopathy-pituitary dysfunction). *Am J Med Genet A* 138A (3), 268–271. doi:10.1002/ajmg.a.30953

Haritoglou, C., Rudolph, G., Kalpadakis, P., and Boergen, K. P. (2003). Congenital trichomegaly (Oliver-McFarlane syndrome): a case report with 9 years' follow up. *Br J Ophthalmol* 87 (1), 119–120. doi:10.1136/bjo.87.1.119

Hufnagel, R. B., Hein, A. G., Arno, N. D., Hersheson, J., Prasad, M., Anderson, Y., et al. (2015). Neuropathy target esterase impairments cause Oliver-McFarlane and Laurence-Moon syndromes. *Journal Of Medical Genetics* 52 (2), 85–94. doi:10.1136/jmedgenet-2014-102856

Hutchison, D. M., Duffens, A., Yale, K., Park, A., Cardenas, K., and Mesinkovska, N. A. (2022). Eyelash trichomegaly: a systematic review of acquired and congenital aetiologies of lengthened lashes. *J Eur Acad Dermatol Venereol* 36 (4), 536–546. doi:10.1111/jdv.17877

Kazanci, S., Witt, J., Su, K., Lorenzo-Betancor, O., Yearout, D., Zabetian, C. P., et al. (2022). PNPLA6-Related disorder with levodopa-responsive parkinsonism. *Mov Disord Clin Pract* 10 (2), 338–340. doi:10.1002/mdc3.13632

Kmoch, S., Majewski, J., Ramamurthy, V., Cao, S., Fahiminiya, S., Ren, H., et al. (2015). Mutations in PNPLA6 are linked to photoreceptor degeneration and various forms of childhood blindness. *Nature Communications* 6 (1), 5614. doi:10.1038/ncomms6614

Lacouture, M. E., Boerner, S. A., and Lorusso, P. M. (2006). Non-rash skin toxicities associated with novel targeted therapies. *Clin Lung Cancer* 8 (Suppl. 1), S36–S42. doi:10. 3816/clc.2006.s.012

Li, H., Ji, C. Y., Zong, X. N., and Zhang, Y. Q. (2009). Height and weight standardized growth charts for Chinese children and adolescents aged 0 to 18 years. *Zhonghua Er Ke Za Zhi 47* (7), 487–492.

Lisbjerg, K., Andersen, M. K. G., Bertelsen, M., Brost, A. G., Buchvald, F. F., Jensen, R. B., et al. (2021). Oliver McFarlane syndrome: two new cases and a review of the

Generative AI statement

The author(s) declare that no Generative AI was used in the creation of this manuscript.

Any alternative text (alt text) provided alongside figures in this article has been generated by Frontiers with the support of artificial intelligence and reasonable efforts have been made to ensure accuracy, including review by the authors wherever possible. If you identify any issues, please contact us.

Publisher's note

All claims expressed in this article are solely those of the authors and do not necessarily represent those of their affiliated organizations, or those of the publisher, the editors and the reviewers. Any product that may be evaluated in this article, or claim that may be made by its manufacturer, is not guaranteed or endorsed by the publisher.

literature. Ophthalmic Genetics 42^* (4), 464-473. doi:10.1080/13816810.2021. 1904419

Liu, J., and Hufnagel, R. B. (2023). PNPLA6 disorders: what's in a name? *Ophthalmic Genet* 44 (6), 530–538. doi:10.1080/13816810.2023.2254830

Liu, F., Ji, Y., Li, G., Xu, C., and Sun, Y. (2020). Identification of Oliver-McFarlane syndrome caused by novel compound heterozygous variants of PNPLA6. *Gene* 761, 145027. doi:10.1016/j.gene.2020.145027

Liu, J., He, Y., Lwin, C., Han, M., Guan, B., Naik, A., et al. (2024). Neuropathy target esterase activity defines phenotypes among PNPLA6 disorders. *Brain* 147 (6), 2085–2097. doi:10.1093/brain/awae055

Luiz Pedroso, J., Rivero, R. L. M., De Miranda, V. A. D., Avelino, M. A., Dutra, L. A., Ribeiro, R. S., et al. (2014). Neuroimaging features in congenital trichomegaly: the Oliver-McFarlane syndrome. *Journal of Neuroimaging* 24 (4), 418–420. doi:10.1111/jon. 12025

Makuloluwa, A. K., Dodeja, R., Georgiou, M., Gonzalez-Martin, J., Hagan, R., Madhusudhan, S., et al. (2020). Oliver McFarlane syndrome and choroidal neovascularisation: a case report. *Ophthalmic Genetics* 41 (5), 451–456. doi:10.1080/13816810.2020.1783689

Mathieu, M., Goldfarb, A., Berquin, P., Boudailliez, B., Labeille, B., and Piussan, C. (1991). Trichomegaly, pigmentary degeneration of the retina and growth disturbances. A probable autosomal recessive disorder. *Genet Couns.* 2 (2), 115–118. PMID: 1781955.

Nedresky, D., and Singh, G. (2022). Physiology, luteinizing hormone. In *StatPearls. Treasure Island, FL: StatPearls Publishing. Available online at: https://www.ncbi.nlm.nih.gov/books/NBK582268/.

Oliver, G. L., and McFarlane, D. C. (1965). Congenital trichomegaly: with associated pigmentary degeneration of the retina, dwarfism, and mental retardation. *Arch Ophthalmol* 74, 169–171. doi:10.1001/archopht.1965.00970040171008

OMIM (2025). Online mendelian inheritance in man. Available online at: https://omim.org/entry/245800.

Ono, T., Taketomi, Y., Higashi, T., Sato, H., Mochizuki-Ono, C., Nagasaki, Y., et al. (2025). PNPLA6 regulates retinal homeostasis by choline through phospholipid turnover. *Nature Communications* 16 (1), 2221. doi:10.1038/s41467-025-57402-8

Patsi, O., De Beaufort, C., Kerschen, P., Cardillo, S., Soehn, A., Rautenberg, M., et al. (2018). A new PNPLA6 mutation presenting as Oliver McFarlane syndrome. *J Neurol Sci* 392, 1–2. doi:10.1016/j.jns.2018.06.016

Patton, M. A., Harding, A. E., and Baraitser, M. (1986). Congenital trichomegaly, pigmentary retinal degeneration, and short stature. *Am J Ophthalmol* 101 (4), 490–491. doi:10.1016/0002-9394(86)90656-2

Richards, S., Aziz, N., Bale, S., Bick, D., Das, S., Gastier-Foster, J., et al. (2015). Standards and guidelines for the interpretation of sequence variants: a joint consensus recommendation of the American college of medical genetics and genomics and the association for molecular pathology. *Genetics In Medicine 17 (5), 405–424. doi:10. 1038/gim.2015.30

Richardson, R. J., Fink, J. K., Glynn, P., Hufnagel, R. B., Makhaeva, G. F., and Wijeyesakere, S. J. (2020). Neuropathy target esterase (NTE/PNPLA6) and

organophosphorus compound-induced delayed neurotoxicity (OPIDN). Adv Neurotoxicol 4, 1–78. doi:10.1016/bs.ant.2020.01.001

Sampson, J. R., Tolmie, J. L., and Cant, J. S. (1989). Oliver McFarlane syndrome: a 25-year follow-up. Am J Med Genet 34 (2), 199–201. doi:10.1002/ajmg.1320340213

Sheng, X., Zhang, S., Boergen, K. P., Li, H., and Liu, Y. (2015). Oliver-McFarlane syndrome in a Chinese boy: retinitis pigmentosa, trichomegaly, hair anomalies and mental retardation. *Ophthalmic Genetics* 36* (1), 70–74. doi:10.3109/13816810.2013. 874003

Shi, J., Zhang, X., Xu, K., Xie, Y., Zhang, X. H., and Li, Y. (2023). A case of Oliver-McFarlane syndrome caused by PNPLA6 gene mutation. *Zhonghua Yan Ke Za Zhi* 59 (6), 484–487. Chinese. doi:10.3760/cma.j.cn112142-20220627-00316

Sonmez, S., Forsyth, R. J., Matthews, D. S., Clarke, M., and Splitt, M. (2008). Oliver-McFarlane syndrome (chorioretinopathy-pituitary dysfunction) with prominent early pituitary dysfunction: differentiation from choroideremia-hypopituitarism. *Clin Dysmorphol* 17 (4), 265–267. doi:10.1097/MCD. 0b013e328306a374

Synofzik, M., Hufnagel, R. B., and Züchner, S. (2014). "PNPLA6 disorders," in *GeneReviews*." Editors M. P. Adam, J. Feldman, G. M. Mirzaa, R. A. Pagon, S. E. Wallace, and A. Amemiya (Seattle (WA): University of Washington, Seattle), 1993–2025.

Topaloglu, A. K., Lomniczi, A., Kretzschmar, D., Dissen, G. A., Kotan, L. D., McArdle, C. A., et al. (2014). Loss-of-function mutations in PNPLA6 encoding neuropathy target esterase underlie pubertal failure and neurological deficits in gordon holmes syndrome. *J Clin Endocrinol Metab* 99 (10), E2067–E2075. doi:10.1210/jc.2014-1836

Wu, S., Sun, Z., Zhu, T., Weleber, R. G., Yang, P., Wei, X., et al. (2021). Novel variants in PNPLA6 causing syndromic retinal dystrophy. *Exp Eye Res* 202, 108327. doi:10.1016/j.exer.2020.108327

Yamamoto, K., Taketomi, Y., Isogai, Y., Miki, Y., Sato, H., Masuda, S., et al. (2011). Hair follicular expression and function of group X secreted phospholipase A2 in mouse skin. *J Biol Chem* 286 (13), 11616–11631. doi:10.1074/jbc.M110.206714

Zaun, H., Stenger, D., Zabransky, S., and Zankl, M. (1984). The long-eyelash syndrome trichomegaly syndrome, Oliver-McFarlane. *Hautarzt* 35 (3), 162–165.

Glossary

OMCS Oliver-McFarlane syndrome
WES whole-exome sequencing
RPE retinal pigment epithelium

GH growth hormone

LH luteinising hormone

FSH follicle-stimulating hormone
TSH thyroid-stimulating hormone
NTE neuropathy target esterase
BNS Boucher-Neuhauser syndrome
GHS Gordon-Holmes syndrome
OMCS Oliver-McFarlane syndrome
LMS Lawrence-moon syndrome

HGMD Human Gene Mutation Database

spastic paraplegia type 39

MRI magnetic resonance imaging
BCVA best-corrected visual acuity
ff-ERG full-field electroretinography
M1 (c.3241G>A, p. Gly1081Arg)
M2 (c.3461G>A, p. Arg1154His)

VF visual fields

SPG39

OCT optical coherence tomography

ACMG College of Medical Genetics and Genomics

OD oculus dexter; OS, oculus sinister

A adenine
Gly glycine
Arg arginine
His histidine

EGFR Epidermal growth factor receptors

LPC lysophosphatidylcholine
PC phosphatidylcholine
GPC glycerophosphocholine